Tellus B
Chemical and Physical Meteorology

Spatio-Temporal Distributions of the Natural Non-Sea-Salt Aerosol Over the Southern Ocean and Coastal Antarctica and Its Potential Source Regions

REVIEW ARTICLE

JOST HEINTZENBERG
MICHEL LEGRAND
YUAN GAO
KEIICHIRO HARA
SHAN HUANG
RUHI S. HUMPHRIES
ADARSH K. KAMRA
MELITA D. KEYWOOD
SERGEY M. SAKERIN

*Author affiliations can be found in the back matter of this article

STOCKHOLM UNIVERSITY PRESS

CORRESPONDING AUTHOR:
Jost Heintzenberg
Institute for Tropospheric Research, Permoserstr. 15, 04318 Leipzig, Germany
jost@tropos.de

KEYWORDS:
Southern Ocean; Antarctica; biogenic marine emissions; aerosol sources; particle number concentrations; particle composition; major ions

TO CITE THIS ARTICLE:
Heintzenberg, J, Legrand, M, Gao, Y, Hara, K, Huang, S, Humphries, RS, Kamra, AK, Keywood, MD and Sakerin, SM. 2023. Spatio-Temporal Distributions of the Natural Non-Sea-Salt Aerosol Over the Southern Ocean and Coastal Antarctica and Its Potential Source Regions. *Tellus B: Chemical and Physical Meteorology*, 75(1): 47–64. DOI: https://doi.org/10.16993/tellusb.1869

ABSTRACT

More than 40 years of aerosol data including concentrations of particle number and of nine major ions collected over the Southern Ocean and coastal stations have been aggregated and filtered with back trajectories to reduce the risk of influence from adjacent continents. That provided a rich dataset including latitudinal distribution and seasonality of physical and chemical aerosol parameters that allow insights into aerosol sources over the Southern Ocean. These data together with statistics of back trajectory paths of high (75% percentile) and low (25% percentile) concentrations of the studied aerosol parameters were used to identify potential source regions of the respective compounds. For particle number concentrations, MSA, and the non-sea-salt fractions of Ca and potassium the most prominent source regions were found in high DMS-areas close to Antarctica, whereas the potential source regions of NH_4 and the non-sea-salt fraction of Mg were located in part further north over the Southern Ocean. These geographical differences would reflect differences in the marine biota.

1 INTRODUCTION

The marine atmosphere over the Southern Ocean and Antarctica, being far from the few adjacent populated continental southern hemispheric land masses, is our closest present-day analogue to the pre-industrial state due to its pristine character (Hamilton et al., 2014). Concerning the regional aerosol these environmental conditions imply lower concentrations of any anthropogenic aerosol components than in the marine atmosphere of the northern hemisphere. Knowledge of the atmospheric composition under such pristine conditions provides a baseline for understanding climate changes in the global warming discussion of the industrial era.

Natural aerosol sources, however, can be very important in this region. Due to the strong and persistent westerlies over the Southern Ocean the mechanical source of sea salt particles dominates particulate mass in the regional marine boundary layer (Gong et al., 1997; Jiang et al., 2021). Furthermore, in the presence of sea ice (Wagenbach et al., 1998), emissions from blowing snow were recently demonstrated to be a significant (possibly dominant in winter) sea-salt source compared to the common sea-salt emissions from the open ocean in the Antarctic regions (Yang et al., 2019; Frey et al., 2020). The increased understanding of the ocean surface microlayer (Riley, 1963; Garrett, 1967; Aller et al., 2005) added a host of biogenic and some enriched inorganic ions to the source of sea salt particles (Leck and Bigg, 1999; Leck and Bigg, 2005).

The high marine primary productivity in surface waters of the Southern Ocean (Westberry et al., 2008) causes very high concentrations of the waste product dimethyl sulfide (DMS) compared to other oceanic regions, (Hulswar et al., 2021), that is vented to the atmosphere. After photooxidation and multiphase oxidation this DMS yields the particulate sulfur components, mainly sulfate and methane sulfonic acid (MSA), (Hoffmann et al., 2016), and is a major regional natural aerosol source. This source exhibits large spatio-temporal and seasonal variability because of the strong dependence of the DMS production in the surface sea waters and related gas-to-particle conversion processes on both oceanic and atmospheric conditions and plays a vital role in the climate system and its variability (Charlson et al., 1987; Andreae and Crutzen, 1997).

Beginning with the discussion of global background or baseline atmospheric parameters in the 1970s, (e.g., Junge, 1972), a number of atmospheric monitoring stations with aerosol programs were established in pristine environments of the Southern Hemisphere. At the same time, geopolitical developments led to a rapidly increasing number of research stations in coastal Antarctica that also established aerosol monitoring. Supply voyages to these Antarctic stations, more recently complemented by an increasing number of research cruises, have greatly increased the geographical coverage of aerosol data over the Southern Ocean. Despite the many technical, logistic and meteorological challenges aerosol measurements have been made in this region for over 40 years. They started from simple electrical and optical methods in earlier years to the present extremely detailed physical and chemical measurements directed at specific aerosol sources and processes (e.g., Alroe et al., 2020; Brean et al., 2021; Sanchez et al., 2021; Simmons et al., 2021; Twohy et al., 2021).

Focusing on Antarctica proper Shaw (1988) provided a first review of aerosol data up to 1987 concluding that most of the Antarctic aerosol is "deriving from biological processes taking place in the surrounding oceans". First synoptic efforts to investigate the combination of chemical aerosol data were made at several Antarctic stations (Wolff et al., 1998; Weller et al., 2011). Combining marine data until the end of the 20th century Heintzenberg et al., (2000) derived latitudinal profiles of particle number concentrations and chemical aerosol information over the remote Southern Ocean. Since then a wealth of new aerosol data have been accumulated at ever more stations and on cruises including the first Antarctic Circumnavigation Expedition directed at the pristine aerosol (Schmale et al., 2019). Also, more detailed oceanographic and biological information has been published (Righetti et al., 2019; Hulswar et al., 2021; Kremser et al., 2021). Thus, a new effort to combine the available aerosol data over the pristine southern hemispheric region seems well motivated. This study aims at a synoptic view of available data on latitudinal and seasonal distributions of key physical and chemical aerosol parameters over the pristine Southern Ocean and coastal Antarctica. The combined statistical data set of the present study comprising more than 40 years of data is useful in future validations of simulations of global physical and chemical aerosol models such as GLOMAP (Spracklen et al., 2005), MOZART (Emmons et al., 2010) or UKESM (Sellar et al., 2019). With air-mass back trajectories these distributions are extrapolated over larger geographical regions to identify of potential natural aerosol source areas. Besides minimizing the contributions of continental aerosol sources by means of trajectory filtering we explicitly exclude the discussion of the source of sea salt particles, (Lewis and Schwartz, 2004). Also, we do not discuss the upper Antarctic atmosphere as potential source for the aerosol of the coastal Antarctic environment. Except for the discussion seasonal distributions of parameters with sufficiently large data base we exclude a discussion of temporal developments due to the inhomogeneity and scarcity of available data.

2 DATABASE

Through literature searches and contact with the responsible scientists, aerosol data from 27 research sites and 23 research cruises have been collected in the data base of the present study. The data have been taken from the literature cited in Table T1. Substantial exceptions are the stations Cape Point, South Africa, and the most recent (> 2019) data from Kennaook Cape Grim, Tasmania, G.v. Neumayer, Antarctica, King Sejong, Antarctica, Syowa, Antarctica, and SHIRASE cruises.

The data comprise coastal and island stations from South Africa to Antarctica and cruises from in Atlantic, Australia/New Zealand, Indian, and Pacific sectors of the Southern Ocean to and around Antarctica. Being situated some 200 km inland the Belgian Antarctic station Princess Elisabeth is the only non-coastal site, which is considered in this study because of its relatively low elevation of 1390 m a.s.l., (Herenz et al., 2019). Despite the many technical, logistic and meteorological challenges aerosol measurements have been made in the study region for over 40 years. They started from simple electrical and optical methods in earlier years to the present extremely detailed physical and chemical measurements directed at specific aerosol sources and processes (e.g., Alroe et al., 2020; Brean et al., 2021; Sanchez et al., 2021; Simmons et al., 2021; Twohy et al., 2021). Our minimum requirement for inclusion in the data base was the availability of exact geolocation and sampling times of the measurements or samplings as far back in time as possible.

In Table T1 the details of the sites and cruises are presented together with relevant citations. The map in Figure S1 displays the cruise tracks of all utilized experiments and the locations of the stations of the present study. Most of the stations and cruises lie in the Atlantic and Indian sector of the Southern Oceans whereas the data coverage is sparser in the Pacific sector. In the discussion of meridional distributions of aerosol properties, the question arises to what extent the particular results in the region between –40° and –60° might be determined by a high geographic data density. Figure S2 shows that this indeed is the case for particle number concentration data (due to the long time series at Kennaook Cape Grim, Tasmania) albeit not for chemical aerosol properties. The temporal coverage also is rather uneven because few research or supply cruises operated in the months May through October. We discuss the problem of local and distant contamination of the data in Section 4 of the Supplement.

2.1 PARTICLE NUMBER CONCENTRATIONS

Total particle number concentration is a key aerosol property. Any experimental values of this parameter strongly depend on the lower and to some extent on the upper size limit of the specific sampling method or air intake. Initially photo-electric condensation particle counters, (CPC's), of the Nolan-Pollak-type were utilized (Nolan and Pollak, 1946) in the present study. Gras et al., (2002) determined their lower cut-off-size to 4 nm through intercomparison of condensation nuclei and aerosol particle counters. With the advent of commercially available single-particle CPC's in the 1980s, the range of utilized aerosol instruments widened rapidly. Cut-off-sizes as low as 3 nm were realized in the TSI-3025 counter (Wiedensohler et al., 1997) and successors, the data of which are named N_3 in this study. However, most frequently the data of the present study are based on counters like the TSI 3760 and its successors, having a higher cut-off-size around 10 nm, named N_{10} in this study. The difference of concurrent measurements with these two types of counters is interpreted as the number concentration between 3 and 10 nm, termed N_{3-10}. In a few experiments CPC data were not available but particle number size distributions were measured (Koponen et al., 2002; Asmi et al., 2010; Huang et al., 2018). In these cases, the size distributions were integrated with the lower cut-off-sizes three and 10 nm to provide comparable results.

2.2 PARTICLE COMPOSITION

The first chemical information of the aerosol over the Southern Ocean was derived in the 1970ties from bulk high volume samples taken for several hundred hours downstream of inlets with undefined or undocumented characteristics. From the 1990s on well-defined inlets with PM10 (particle diameters less than 10μm) or even PM2.5 (particle diameters less than 2.5μm) characteristics were deployed increasingly even at remote sites (e.g., Keywood et al., 1999). Improved analytical refinements allowed daily low-volume samples. Today aerosol mass spectroscopy (AMS) yields temporal resolutions of less than one hour for a wealth of organic and inorganic particulate components. AMS typically has an upper size limit of one micrometer.

For the sake of a synopsis of all historical information on the natural aerosol over the Southern Ocean we utilized in the present study historical samples without well-defined sampling characteristics as well as later and recent more size-characterized samples. Mass concentrations of the nine most major ions most frequently analyzed by ion chromatography were collected in the data base (sodium, ammonium, potassium, magnesium, calcium, MSA, chloride, nitrate, and sulfate).[1] They were complemented with the non-sea salt (nss) parts of sulfate, potassium, magnesium, and calcium when sodium values were available as seawater reference ion (Stumm and Morgan, 1981). AMS data were averaged over one-hour periods. Sub-micrometer or PM2.5-inlet derived data were combined with parallel super-micrometer samples. Nevertheless, there are remaining inherent uncertainties when comparing strongly wind-speed dependent sea salt components taken at different wind speeds and heights over the sea surface or distances from the shoreline with different samplers.

For the interpretation of the aerosol data hourly ten-day air-mass back trajectories were calculated arriving at 300 m over the sampling points. The trajectories cover each hour of the collected physical and chemical aerosol data. Details of the trajectory calculations can be found in Section 3 of the Supplement.

2.3 DIMETHYL SULFIDE

As a by-product of the life cycle of phytoplankton dimethyl sulfide (DMS) is released from the oceans to the atmosphere (e.g., Simó, 2001). After photooxidation DMS provides a major natural source of sulfurous particulate matter in the atmosphere (Charlson et al., 1987). Thus, the spatio-temporal distribution of DMS is of relevance for our study of natural aerosol sources over the Southern Ocean. The climatology of atmospheric DMS is, however, only available at Amsterdam Island (Sciare et al., 2000) and Dumont d'Urville (Preunkert et al., 2007) and we here utilize the distribution of DMS in surface sea water as a proxy of atmospheric DMS. The most recent climatology of this parameter has been published by Hulswar et al., (2021). In this study we compare its monthly distributions in different latitude bands with the collected aerosol data over the Southern Ocean.

An alternative proxy for measured atmospheric DMS concentration could have been modeled air concentrations taken from a global atmospheric model such as presented by Chen et al., (2018). For two reasons we chose not to follow this path. One, the output of an atmospheric model over Southern Ocean and Antarctica suffers from the same meteorological data sparseness as back trajectories. Two, the seawater DMS climatology used in this model does not reflect the recent data improvements, in particular over the Southern Ocean, that the DMS climatology by Hulswar et al., (2021) used in the present study.

3 DISCUSSION OF RESULTS

The discussion of results proceeds from latitudinal to seasonal distributions and from there to extrapolated data in the form of maps. Despite our efforts to select comparable measurements the content of our database is highly inhomogeneous. Concerning particle number concentrations inlet losses, sensor principles and sensitivities, evaluation algorithms, and particle size limits varied. Concerning particle composition again inlet characteristics and sampling conditions and efficiencies, particle size limits, and analytical procedures varied. Consequently, we consider thorough statistical tests inadequate for the discussion. Instead most results are presented in the form of arithmetic means and medians, the latter complemented by Median Absolute Deviations (MAD) from the medians.

Over the open sea and near ice-free coasts sodium chloride (NaCl) dominates marine particulate mass concentrations. As the source processes of this aerosol components are well understood and incorporated in global models, (Lewis and Schwartz, 2004), we will not discuss it further in detail here. Also, as this mostly super-micrometer-sized component is strongly wind-dependent, samples taken with different samplers on different platforms and at different sites are difficult to compare. We note that on annual average sodium and chloride concentrations of the present data base show prominent maxima of two to six μgm^{-3} in the latitudinal range of strongest storm activity 30° to 60° south. Annual average and median meridional distributions of Na and Cl are shown in Figure S4, with the caveat of potential chlorine loss affecting the concentrations of Cl as previously seen at numerous remote oceanic regions (Kritz and Rancher, 1980; Ayers et al., 1999) as well as at coastal and inland Antarctica (Maenhaut et al., 1979; Legrand et al., 2017).

Until the advent of in situ aerosol mass spectroscopy (e.g., McMurry, 2000) with temporal resolutions of less than one hour aerosol sampling in pristine environments for chemical analyses often required sampling times of more than 100 hours. Under such conditions at the non-Antarctic coastal (Cape Point, South Africa) or island stations near populated continental regions (Kennaook Cape Grim, Tasmania) very few samples were taken without any influence from the nearest continent, i.e. without any hourly back trajectory hitting the nearest continent during a sampling period. At Cape Point we thus excluded the sulfate results from our study. For the very long chemical time series at Kennaook Cape Grim, MSA data were available. With these data combined with a contamination risk derived from hourly back trajectories during the sampling periods we calculated monthly correction factors for nssSO4 according to a procedure that is detailed in Section 2 of the Supplement.

3.1. MERIDIONAL DISTRIBUTIONS

3.1.1 Particle composition

After sodium chloride, sulfate comprises the second most prominent particulate mass fraction of the aerosol. Expressed as $nssSO_4$ Figure 1 shows annual average and median meridional distributions of this component. While we expect contributions from the oxidation of oceanic DMS-emissions, its general trend of decreasing concentrations with increasing southern latitude corresponds to the picture of decreasing anthropogenic influence on the marine aerosol with increasing distance from the major continental sulfur sources. Non-sea-salt potassium (nssK) is plotted for comparison in Figure 1 because this component also is strongly influenced by continental anthropogenic (or natural) combustion sources (Virkkula et al., 2006b; Hara et al., 2019). The

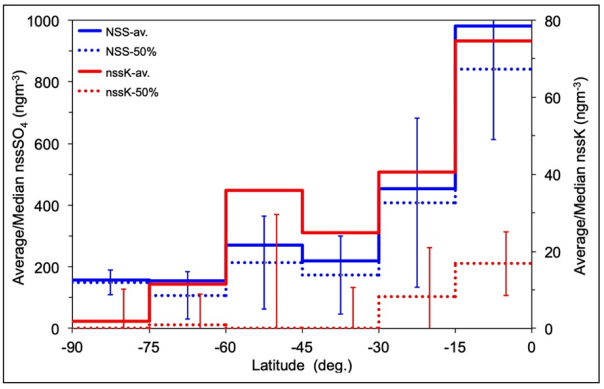

Figure 1 Annual average (av.) and median (50%) meridional distributions of $nssSO_4$ (NSS), and nssK, both in ngm^{-3}. The error bars represent corresponding MAD values.

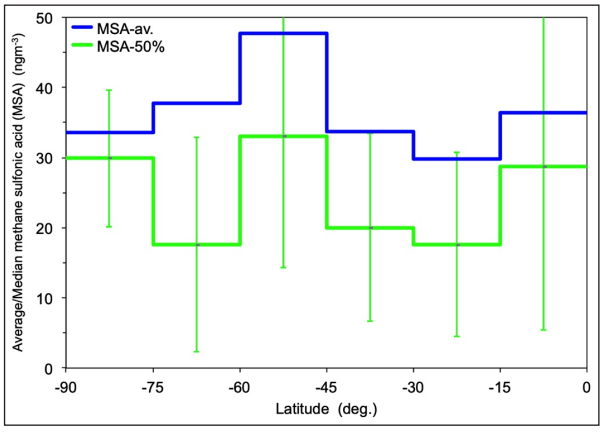

Figure 2 Annual average (av.) and median (50%) meridional distribution of methane sulfonic acid (MSA) in ngm^{-3}. The error bars represent corresponding MAD values.

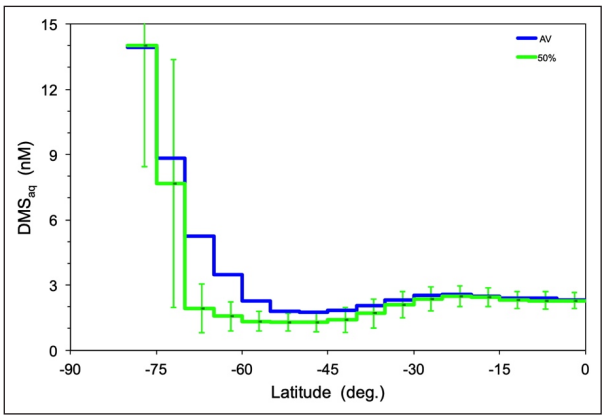

Figure 3 Annual average (av.) and median (50%) meridional distribution of dimethyl sulfide (DMS_{aq}, nM) in surface sea water from Hulswar et al., (2021). The error bars represent corresponding MAD values.

continuous decrease of nssK with increasing southern latitude confirms the nature of a pristine southern marine atmosphere. The differences between means and medians in Figure 1 are worth mentioning. For nssK they imply that the relatively high means are due to rather infrequent events, in the line of the expected sporadic presence of biomass burning plume debris over the Southern Ocean (Giglio et al., 2013). For $nssSO_4$ the means and the high MAD-values in the latitude range –45° to –60° indicate either the possibility of another regional non-combustion source of sulfate or strengthened DMS-emissions.

In contrast to $nssSO_4$, the annual average meridional distribution of MSA (Figure 2) reveals no decreasing trend with increasing latitudes. These differences in the meridional distributions of the two by-products of DMS-oxidation, already observed during several cruises (Bates et al., 1992; Virkkula et al., 2006a; Virkkula et al., 2006b), confirm the importance of non-DMS source of sulfate over most of the low- and mid- latitude Southern Ocean. In comparison to the distribution of $nssSO_4$ the rather flat, (±20%), annual average meridional distribution of MSA only reveals a weak maximum of 48 ngm^{-3} in the latitude range –45° to –60° with a shoulder towards Antarctica.

Whereas this meridional maximum of MSA is co-located with that of $nssSO_4$ with potential biological causes (see also further discussions on nssCa and nssMg), it does not correspond to the distribution of its gaseous precursor DMS. Conversely, annual average and median meridional distributions of DMS in surface sea water in Figure 3[2] have broad minima between –40° and –60° increasing south of the polar front to extremely high values towards Antarctica. Interestingly however, the region around –45° has been shown to exhibit a hemispheric maximum in plankton species turnover and a minimum in plankton species richness, (Righetti et al., 2019). The same latitude band exhibits maximum net primary production, (NPP), with the highest seasonal variability in NPP in the southern hemisphere, (Righetti et al., 2019; Henley et al., 2020). Furthermore, possibly even more important, the ocean-air flux of DMS is expected to be strengthened in this –40° to –50° latitude belt due to high wind speeds (cf. Bates et al., 1992). Finally, the absence of an increase in MSA <–65° that contrasts with the occurrence of a maximum of the DMS_{aq} precursor suggests important effects of other parameters such as wind speed and atmospheric photochemistry (different atmospheric residence times of DMS and MSA). As discussed in Section 3.2.1, differences can also be observed in the seasonal cycle of DMS_{aq} with respect to those of atmospheric MSA and $nssSO_4$.

The two components nssCa and nssMg in Figure 4 exhibit an anomaly in the latitude range –45° to –60°. Although being abundant in atmospheric dust, these two components likely do not originate there from dust emissions since their high levels of nssCa and nssMg remain when coastal and island data are eliminated from the dataset. The –45° to –60° latitude belt represents the so-called storm track area, where strong emissions of sea-salt aerosols by the bubble bursting mechanism take place. In this latitude range both, averages and medians of nssCa and mean nssMg-data reach absolute maxima (see Figure 4).

High values of nssCa in marine aerosols have been reported from many laboratory and field studies (Hoffman and Duce, 1977; Weisel et al., 1984; Keene et al., 2007; Jayarathne et al., 2016; Salter et al., 2016; Mukherjee et al., 2020). The enrichment relative to the bulk seawater composition is attributed to the divalent ions Ca^{2+} and Mg^{2+} residing complexed in the polymer gels of the ocean surface microlayer (OSM), (Chin et al., 1998), fragments of which are emitted together with sea salt emissions, which are highly efficient in the storm region over the Southern Ocean. Mg in the sea salt aerosol can also be enriched by sea salt fractionation on sea ice. Near the Antarctic coast most of sea-salt aerosol, at least in winter, is released from the sea-ice surface as shown in Hara et al. (2020), and references therein. The strength of the OSM is strongly coupled to the seasonally variations of the ecology of the underlying water column (Dreshchinskii and Engel, 2017). For nutrient chemicals maximum enrichments in the OSM have been reported at times of maximum biological activity (Lyons and Pybus, 1980). Note that, contrasting with the case of divalent cations, nssK does not exhibit any anomaly in the southern midlatitude range (see Figure 1). This difference between NssK and NssCa and NssMg is in the line of results from laboratory experiments with sea water yield enrichments showing a far weaker (or an absence of) enrichment for potassium than for divalent cations (Jayarathne et al., 2016).

Ammonia (NH_3) and its protonated form ammonium (NH_4^+) are produced in surface sea water by the biological reduction of nitrate (either directly or via the degradation of biologically synthesized organic nitrogenous material) (Johnson et al., 2008). Large bird colonies on remote islands and coastal regions of the Southern Ocean provide additional strong sources of ammonia (Legrand et al., 1998; Schmale et al., 2013). A 'co-production' of NH_3 and DMS has been hypothesized by Quinn et al., (1990) and Liss and Galloway (1993), albeit challenged and proposed instead as a DMS-driven 'co-emission' of ammonia by Johnson et al., (2008). For the present study, ammonium data are also relevant because its gaseous NH_3 precursor has been recognized to act as a facilitating agent in atmospheric new particle formation via the nucleation of sulfuric acid, (e.g., Curtius, 2006).

Figure 5 shows annual average and median high NH_4 concentrations co-located with the tropical and mid-southern latitude regions with high NH_3-emissions from the ocean in accordance with a review of global experimental and model results (Paulot et al., 2015).

In addition to NH_4 concentration changes with latitude, the meridional distribution of the $NH_4/nssSO_4$ molar ratio provides information on (1) the degree of neutralization of submicron aerosol and (2) the magnitude of NH_3 oceanic emissions. Indeed, away from continents where large emissions of calcium carbonates sometimes take place, sea-salt associated cations and ammonium are the most important cations controlling the acidity of atmospheric aerosol. Chemical size distribution have shown that, over the Southern Ocean, ammonium mainly stays together with $nssSO_4$ in submicrometer particles, where the amount of alkaline sea-salt is not high enough to compete with NH_3 in neutralizing H_2SO_4, (Virkkula et al., 2006a; Xu et al., 2013; Weller et al., 2018). In the remote marine aerosol, Quinn et al., (1990) reported mean $NH_4/nssSO_4$ molar ratios of ~1.3, indicating only partly neutralized sulfate particles. If confirmed, these findings imply that most NH_x (NH_3 plus NH_4) is there in the form of NH_4. Under these conditions, the $NH_4/nssSO_4$ molar ratio is sensitive to NH_3 emissions and can be used to constrain models dealing with NH_3 and DMS marine emissions, (Paulot et al., 2015).

Previous studies of the meridional change of R_m, are very rare and were mainly obtained during short summertime ship traverses in the Southern Ocean, (Paulot et al., 2015). One study reported a gradient of the $NH_4/NssSO_4$ molar ratio from 0.06 at 70°S to 0.6 between −60° and −65°, and ~1.0 north of −60° (O'Dowd et al., 1997). As done by Legrand et al. (2021)in evaluating the state of neutralization of the Antarctic aerosol, we here included MSA to calculate the $R_m = NH_4/(nssSO_4 + MSA)$ molar ratio.

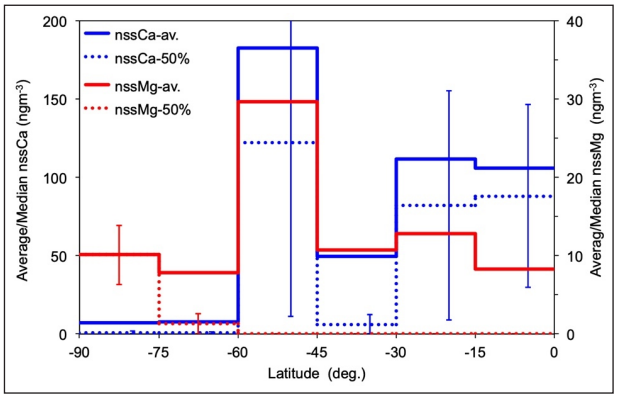

Figure 4 Annual average (av.) and median (50%) meridional distributions of nssCa, and nssMg, both in ngm^{-3}. The error bars represent corresponding MAD values. North of −60° median values of nssMg are zero.

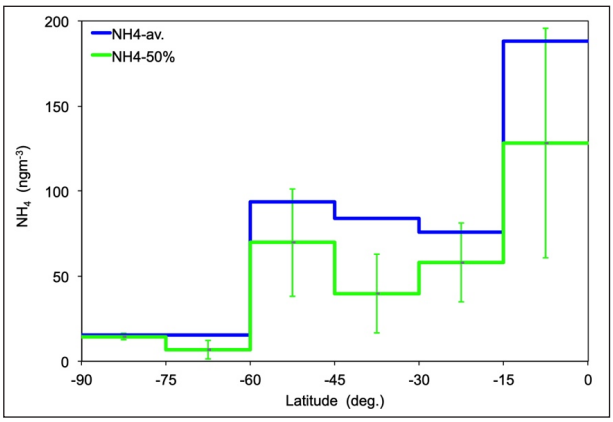

Figure 5 Annual average (av.) and median (50%) meridional distribution of ammonium (NH_4) in ngm^{-3}. The error bars represent corresponding MAD values.

Figure 6 we display mean and median meridional distributions of R_m over the Southern Ocean confirming earlier results of an only partially neutralized submicron aerosol. Due to the large presence of penguin colonies at the site, the strongly locally controlled ammonium data from station Dumont d'Urville (Legrand et al., 1998) have been excluded as an outlier. The most complete particle neutralization by NH_3 is observed in the latitude band –30° to –60° where NH_4 concentrations are the highest.

3.1.2 Particle number

Particle number concentrations N_{10}, and N_{3-10} are controlled by source and aerosol evolution processes yielding nucleating low-vapor pressure gases such as sulfuric acid from photochemical DMS-oxidation (Hoffmann et al., 2016), potentially also by primary particles from the ocean surface microlayer (Leck and Bigg, 1999). Thus, natural aerosol source processes over the Southern Ocean may control the concentrations of N_{10}, and N_{3-10}. At Kennaook Cape Grim this connection between DMS, $nssSO_4$, MSA, and particle number concentrations has been well established experimentally (Ayers and Gras, 1991; Ayers et al., 1991; Ayers et al., 1995; Ayers et al., 1997). In Figure 7 annual average and median meridional distributions of N_{10}, and N_{3-10} are collated. Average N_{10} shows a broad maximum similar to that of MSA with a peak between –45° and –60°, close to the corresponding maximum in the –30° to –45° range that was identified in a previous review, (Heintzenberg et al., 2000). Median N_{10} has a narrower maximum in the –45° and –60° range with high MAD-values. Median N_{3-10} values are generally less than 10% of the corresponding N_{10}-values. However, the lowermost latitudinal bin with data between –60° and –75° however, is an exception. Here relatively high average N_{3-10} values appear, albeit based on a single research cruise in spring 2012, (Humphries et al., 2016).

The infrequent occurrence of particles below 10 nm in the marine atmospheric boundary layer over the Southern Ocean confirms the results of an earlier general review of the marine aerosol, in which particles below 10 nm were found in only 3% of all data (Heintzenberg et al., 2004). Several models have been advanced to explain the persistent number concentrations of these particles around 300 cm^{-3} in the marine boundary layer despite low probability of locally formed particles (Pirjola et al., 2000). In the tropical to subtropical region these models involve the strong convective transport of boundary layer precursor gases into the photochemically active upper troposphere, with subsequent particle nucleation (Raes, 1995; Shaw et al., 1998), from which the aged particles subside into the boundary layer. At Kennaook Cape Grim Gras et al., (2009) suggested this subsidence was related to the passage of fronts (post frontal subsidence). In higher latitudes, warm conveyor belts and sub-polar vortices explain the upward transport of particle precursors. McCoy et al., (2021) summarized the present understanding of the different mechanisms of particle formation over the Southern Ocean and provide new experimental evidence for the nucleation in the free troposphere based on the 2018 SOCRATES aircraft campaign. Recent results with more sensitive instrumentation indicate more frequent new particle formation processes in the marine boundary layer than previously seen (Peltola et al., 2022).

3.2 SEASONAL DISTRIBUTIONS

3.2.1 Particle composition

Seasonal distributions of the data are discussed next. All graphs are centered around the austral summer months December/January. The sparseness of aerosol data cover allows only a broad geographical resolution. We divide the Sothern Hemisphere into two regions, the Antarctic region to south of –65° latitude, from the rest of the hemisphere north of –65°. Consistent with regional aerosol studies (Humphries et al., 2016) and rare atmospheric DMS-data of Koga et al., (2014) this latitude was chosen to

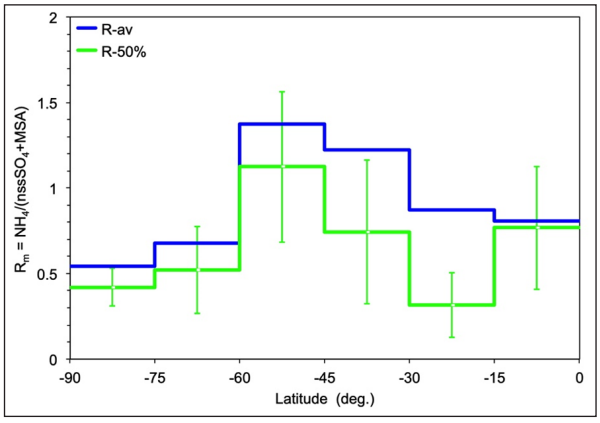

Figure 6 Annual average (av.) and median (50%) meridional distributions of the molar ratio Rm = NH_4/($nssSO_4$+MSA). The error bars represent corresponding MAD values.

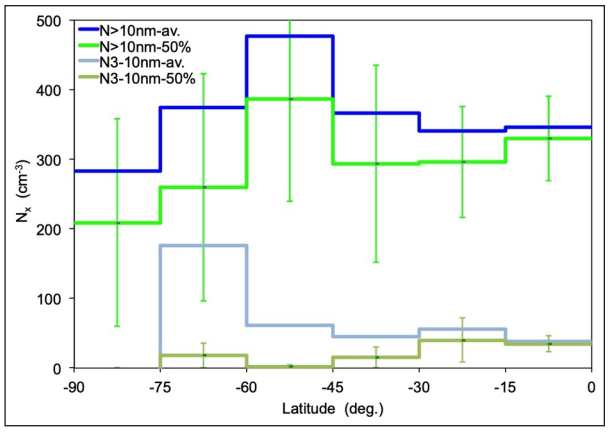

Figure 7 Annual average (av.) and median (50%) meridional distributions of particle number concentrations >10 nm, (N_{10}, cm^{-3}), and between 3 and 10 nm, (N_{3-10}, cm^{-3}). The error bars represent corresponding MAD values.

correspond roughly to the Antarctic circle while enclosing most of the Antarctic coastal and island sites of the present study. Based on the climatological DMS_{aq} of Hulswar et al., (2021) Figure 8 shows the climatological monthly medians ±MAD of DMS_{aq} in surface sea water of the two regions. Whereas monthly winter medians are rather similar in the two regions (~1 nM), monthly summer medians in the Antarctic region are four times higher than further north. As a result, the seasonal cycle in the Antarctic region is more well-marked (a factor of 27 between maximum and minimum values instead of a factor of 3 further north). We note the extremely low winter-MAD-values in the Antarctic region. These spatio-temporal variations of DMS in seawater are controlled by various processes that remain poorly understood including not only phytoplankton biomass but also ecological and biogeochemical processes driven by the geophysical context (e.g., Simó, 2001). As mentioned in Section 3.1.1., the concentrations of atmospheric DMS are not only controlled by DMS_{aq} but also through wind speed affecting the ocean-to-air fluxes.

The seasonal distributions of $nssSO_4$ and MSA in Figure 9 to some extent reflect the meridional variation of DMS_{aq} in seasonality, characterized by strong summer maxima including the earlier onset of concentration increases that is also seen in Figure 8. In the Sub-Antarctic and Polar Antarctic zones defined in Arteaga et al., (2020) the plankton blooming phases begin already in July and peak in biomass in November (Llort et al., 2015). Peak summer-values of MSA and $nssSO_4$ are similar in the two regions (50 – 60 ng m^{-3} and ~300 ng m^{-3}, respectively). In winter MSA exhibits extremely low values in the two regions (1 ng m^{-3} at >–65, 3 ng m^{-3} at <–65°), but the summer-to-winter drop of $nssSO_4$ is more significant at high latitudes. One possibility is that the contribution of anthropogenic sulfate is still significant at latitudes > –65°, but is much weaker at < –65°. North of the Antarctic region Figure NSSMSA indicates a season-independent "background level" of some 100 ngm^{-3} $nssSO_4$ over the pristine Southern Ocean. It is possible that the filtering process described in Section 2 was not sufficient to remove contaminated data, however removing the constraint of requiring at least five days of back trajectories to the nearest continent did not significantly increase this $nssSO_4$ "background level", albeit with a strong rise in MAD-values.

The seasonal distributions of ammonium in Figure 10 also show strong summer maxima in both geographical regions. North of –65°, however, NH_4-concentrations rise earlier (November) than further south and exhibit a secondary maximum in fall (March, April). Because of the strong summer NH_4-peak one might expect that this maximum causes a maximum in particle neutralization in terms of the molar ratio R. However, this is not the case. Because of the comparable or even stronger summer increase in acidifying sulfuric and methane sulfonic acid

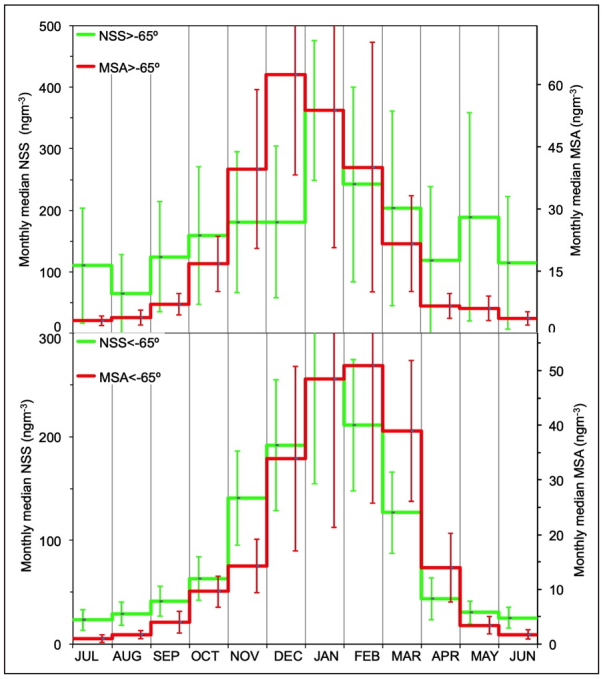

Figure 9 Top: $nssSO_4$, (NSS, ngm^{-3}) and methane sulfonic acid, (MSA, ngm^{-3}) north of –65° latitude. Bottom: Same but south of –65° latitude. The error bars represent median absolute deviations. The scales for MSA were chosen to align January values of NSS and MSA.

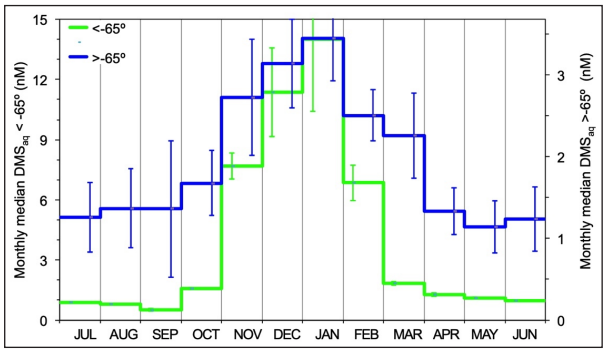

Figure 8 Monthly median DMS_{aq} in surface sea water (nM) of the Southern Ocean south and north of –65° latitude, based on the climatology of Hulswar et al., (2021). The error bars stand for median absolute deviations. The scales for the two regions were chosen to align January values.

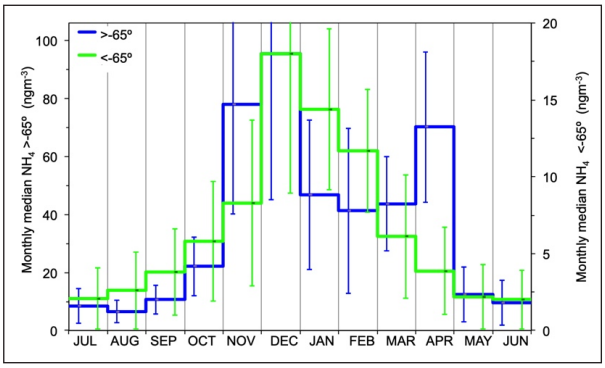

Figure 10 Monthly median ammonium concentrations, (NH_4, ngm^{-3}) north of –65° latitude. Bottom: Same but south of –65° latitude. The error bars stand for median absolute deviations. The scales were chosen to align December values in both regions.

particles the aerosol remains acidic in both regions. South of –65° even the annual minimum of R occurs in summer with a median value of R ≈ 0.3 in February. Again, the strongly locally controlled ammonium data from station Dumont d'Urville have been excluded. In this region the occurrence of an NH_4 maximum in December compared to a $nssSO_4$-maximum in January is consistent with diatom blooms producing NH_3 (Johnson et al., 2008) being one month ahead of phaeocystis blooms producing DMS in the Southern Ocean (Alvain, 2005).

The examination of the seasonal cycle of nss-cations included latitudes south of –45° to incorporate the annual meridional maxima shown in Figure 4. In Figure 11, the three nss fractions exhibit different seasonal variations. NssK shows highest values in summer with a first peak in November and the absolute maximum in January. The November peak might suggest a biomass burning source for this species, as discussed in Section 3.1.1. In terms of medians this peak is most clearly expressed. The timing of arrival of biomass burning debris at latitudes <–60° is indeed consistent with black carbon observations made at Neumayer Station, Antarctica, showing a broad maximum in October-November when the long-range transport of biomass burning debris from South America were able to reach coastal Antarctica at the end of the austral winter, when the isolation from mid latitudes of the Antarctic continent ends (Weller et al., 2013; Hara et al., 2019). As reported by Legrand et al.(2021), the arrival of biomass burning debris in spring seems to be a general feature at coastal as well as inland Antarctica. To test this explanation, we eliminated the five-day threshold in air-mass back trajectories, thus allowing air mass transport from nearby continents within five days, albeit with no significant effects on averages and medians of nssK. As alternative or complementary explanation for the course of the nssK seasonal cycle, in particular for the main summer peak, we offer the emissions from the extensive distribution of macroalgae around Antarctica (Wulff et al., 2009) as a contributor to nssK.

On one hand, the summer maximum of nssCa corresponds to its marine biological source in the OSM (cf. section 3.1.1). We note a trend in the monthly averages of nssCa towards the absolute maximum in March that may be caused by dissolution processes in the OSM at the end of the biologically productive period. As the monthly medians of nssCa do not show this trend the trend in averages may be caused by an increasing number of high-value events that are not reflected in the medians. On the other hand, nssMg that also has been found to be enriched in the OSM does not show a clear summer maximum, (with the possible exception of a small December peak). Monthly averages of nssMg in Figure 11 may even indicate a winter maximum. As an aside, total Magnesium does not show a significant seasonal variation either with the exception of March when the absolute maximum of monthly averages occurs with 56 ngm^{-3}.

3.2.2 Particle number

In both regions, the particle number concentrations N_3 and N_{10} in Figure 12 exhibit broad summer maxima, albeit with more structure south of –65° than further north. The October peak in N_3 is exclusively due to the SIPEX-II cruise in spring 2012, (Humphries et al., 2016). The high MAD-values in September may indicate sporadic NPF-events in early spring as reported by Giordano et al., Lachlan-Cope et al., (2020), and Hara et al., (2021). Aside from these events the absolute annual maxima south of –65° in both size ranges occur in late summer or fall (February/March). In this region, extremely high MAD-values during the two months of September and April indicate frequent events with exceptionally high number concentrations,

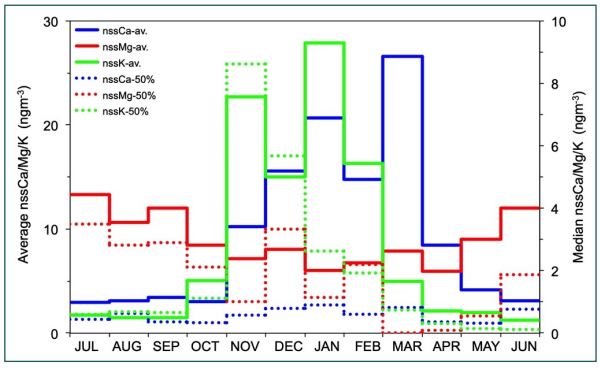

Figure 11 Monthly average and median concentrations of nssCa, nssMg, and nssK, in ngm^{-3} south of –45° latitude. Note the different scales for averages and medians.

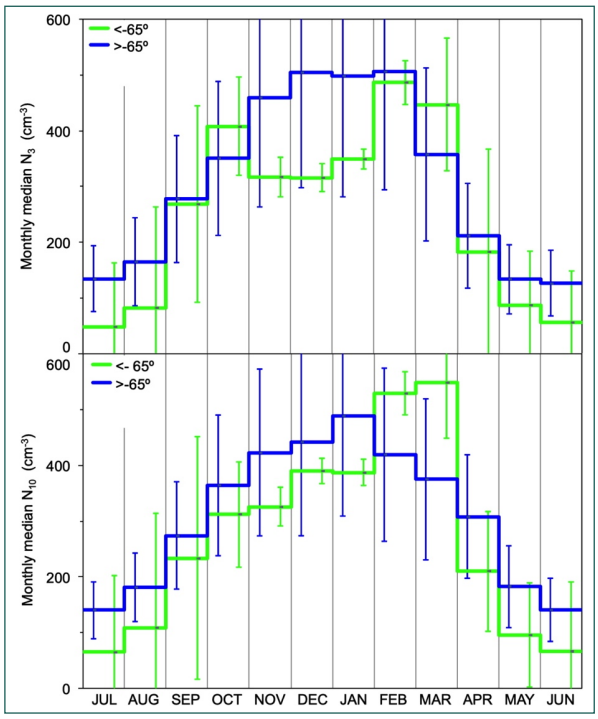

Figure 12 Monthly median number concentrations north and south of –65° latitude. Top: (N_3, cm^{-3}). Bottom: (N_{10}, cm^{-3}). The error bars stand for median absolute deviations.

mostly in N_3 but to some extent visible in N_{10} as well. There are seasonal changes in the air masses reaching the Antarctic coast elated to the variations in the Zonal Wave 3 (ZW3, Raphael, 2007), related to the Semiannual Oscillation, (SAO, van Loon, 1967). ZW3 is a pattern of three climatological low-pressure centers: over the Amundsen Sea, eastern Weddell Sea, and Indian Ocean south of Australia. The SAO causes a strengthening of the meridional pressure gradient between mid-latitudes and Antarctica in spring and autumn, which results in strengthened transport of airmasses from the lower, biologically active latitudes, towards Antarctica.

3.3 POTENTIAL SOURCE REGIONS OF THE NATURAL AEROSOL OVER THE SOUTHERN OCEAN

In the last part of the discussion we identify potential source regions of the natural aerosol over the Southern Ocean. As before, even though wind speed to a large extent controls sea-air fluxes, the climatology of DMS in surface seawaters from Hulswar et al., (2021) is used to start the data discussion. Focusing on the biologically and photochemically most active period, we report in Figure 13 the average distribution of DMS_{aq} between October and April. Statistics of the analyzed aerosol parameters during this period are collected in Table T2. Several distinct features of the DMS_{aq}-distribution can be seen. Due to the high productivity in the many polynyas, (Arrigo and Dijken, 2003), high DMS_{aq}-values are found all around the Antarctic coast. Three hot spots with the highest DMS_{aq}-concentrations show up in Weddell Sea, around the Prydz Inlet, and – with absolute maxima – in the largest polynya in the Ross Sea. The High Nutrient Low Chlorophyll (HNLC) region between –40° and –60° that showed up with minimum DMS_{aq} in Figure 3, is visible as a broad belt all around Antarctica with a few weak interruptions that may be due to the high data density on the most frequent shipping routes to Antarctica. High DMS_{aq}-values also stand out in the map in the west of the southwestern corners of both South America and Africa. Near the latter continent the high values even increase into the street between Africa and Madagascar. North of the belt of minimum DMS_{aq}-values the Southern Atlantic and much of the Southern Pacific exhibit low DMS_{aq}-values whereas higher values are reported for the Indian Ocean. These DMS_a distributions could contribute to the spatio-temporal distributions of particulate biogenic sulfur- in the marine atmosphere over the Southern Ocean.

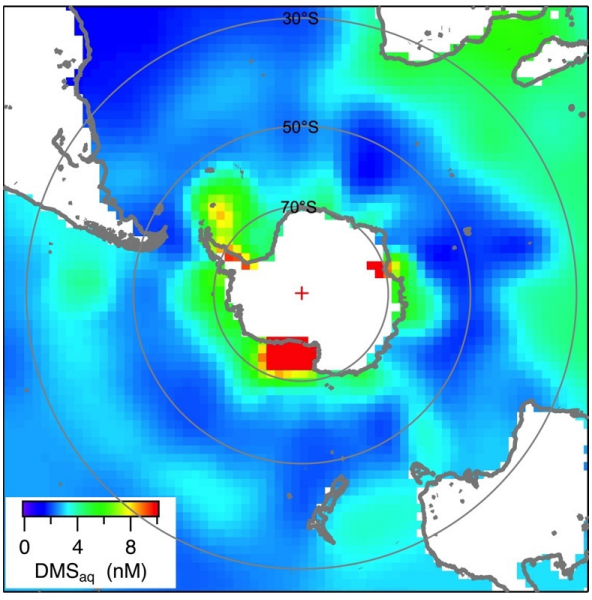

Figure 13 Average distribution of DMS_{aq}, (nM), in surface waters of the Southern Ocean during the months October through April.[3]

Information on the potential aerosol source regions may be inferred from the mapped distributions of air-mass back trajectories from aerosol sampling sites during given sampling times. The maps comprised 14x14 geocells of equal projected size on a stereographical projection of the Southern Hemisphere centered on the South Pole. Hourly hits of back trajectories were counted in each of these geocells. Assuming that the highest values of any aerosol data were most clearly connected to an aerosol source region we summed up trajectory hits in maps for all component values above the respective global 75th percentile. As references we constructed corresponding maps for all component values up to the respective 25th percentile. These two maps for each component comprised 25% each of the data. To compare two maps with different numbers of trajectories we normalized each map with its respective total number of trajectory points. The normalized values in each geocell of the 75%-map ($nrT_{>75\%}$) were then divided by the normalized values of the respective ≤25%-map, ($nrT_{\leq 25\%}$), forming the ratios termed RX, RX = ($nrT_{>75\%}/nrT_{\leq 25\%}$), with X being any of the studied chemical and physical aerosol parameters. The RX-ratios were plotted in color-scale on component maps shown in Figure 14. RX-ratios slightly above zero (blue) indicate that the back trajectories of data above the 75%-level much less frequently hit the respective geocell than for data at median level or below. Ratio values of one (green) indicate that back trajectories of data above the 75% level equally frequent hit the respective geocell as for data at the 25% level or below. Finally, red-colored geocells indicate that the high level data hit the respective geocell twice as frequently or more often than in the respective reference case. These maps presented below are based on the following statistically constraints:

1. All back trajectories within any utilized sample time window or hourly particle number data stay at least 120 hours off the nearest non-Antarctic continent.
2. The positions of the hourly trajectories are traced on maps 120 hours back in time.
3. North of Antarctica only trajectory points below 1000 m above sea level are considered.
4. Only geocells with at least 1000 data points in at least 10 different years are accepted. The long

sampling times of the chemical parameters implied many more hourly trajectories than the hourly CPC-data in the respective maps. Thus, the year-threshold could be raised to 15 years in Figure 14.

MSA exhibits a large compact potential source region in Figure 14 over Dronning Maud Land and Haakon VII Sea with a small secondary peak over the eastern Dumont D'Urville Sea. It covers a region north of the Antarctic coast in the Atlantic and Indian sectors extending from the Falkland Islands towards Marion Island.

Potential source regions for $nssSO_4$ in Figure 14 are less well defined but more clearly two-pronged than for MSA. Less strongly expressed they cover the same Atlantic and Indian regions as for MSA. Ross Sea and vicinity do appear as potential source of secondary magnitude for both. The latter region also shows up as a secondary potential source for nssCa and nssMg in Figure 14. In the broad belt of reemitted dust between –40° and –60° simulated by Cornwell et al., (2020) with the Community Atmospheric Model, Version 5 (CAM5), several hot emission spots show up in this region. The regions extending over Mawson and Davis Sea and much of the ocean south of Australia this area also are the major potential source region for nssK in Figure 14 with a smaller one over Weddell Sea and Bransfield Strait. Finally, for ammonium in Figure 14 a large ring-shaped potential source region surrounds much of Antarctica between –50° and –65°.

The most pronounced potential source regions for particles larger than 3 nm (N_3) is found in Figure 15 in

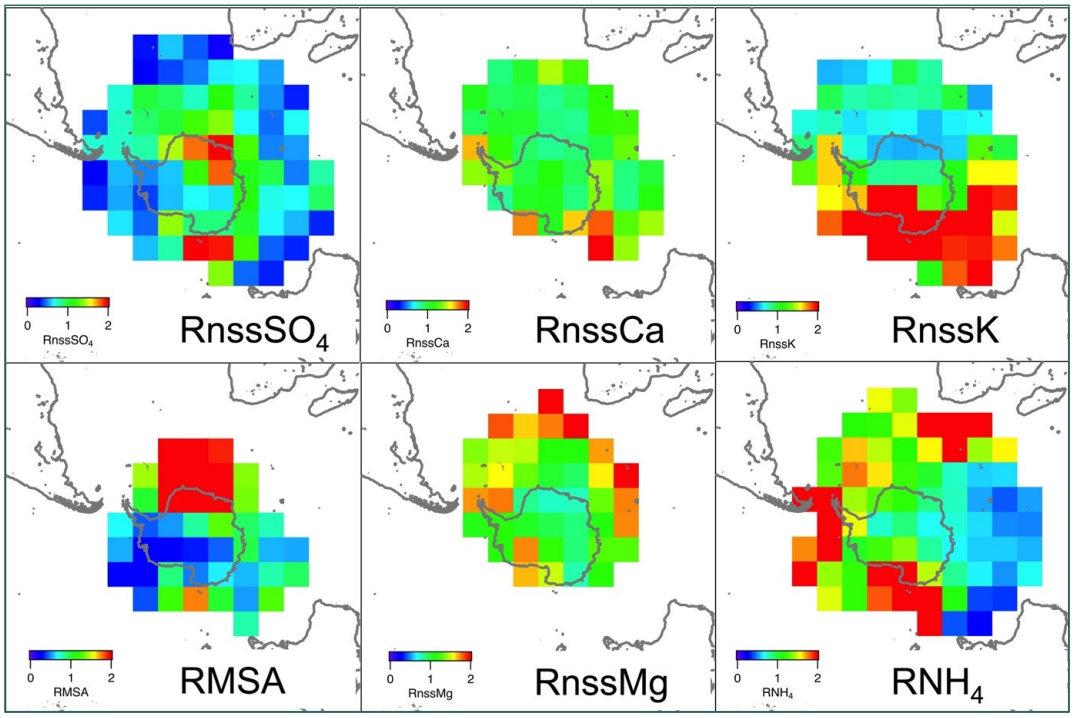

Figure 14 Ratio RX = ($nrT_{>75\%}/nrT_{\leq 25\%}$) of the relative number of trajectory hits for chemical aerosol sample values over the 75%-percentile to that for sample values ≤25%-percentile for the parameters $nssSO_4$, nssCa, nssK, MSA, nssMg, and NH_4 during the months October through April. See text for details about ratio RX.

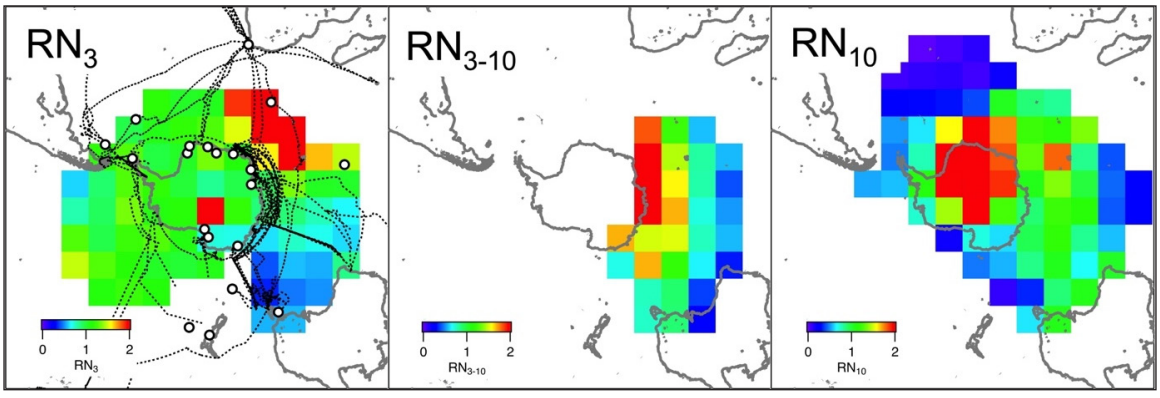

Figure 15 Ratio RX = ($nrT_{>75\%}/nrT_{\leq 25\%}$) of the relative number of trajectory hits for particle number concentrations values over the 75%-percentile to that for sample values ≤25%-percentile for the parameters N_3, N_{3-10}, and N_{10} during the months October through April. See text for details about ratio RX. Circles denote stations, dashed black lines show cruises from which data were used in this study.

the Indian sector of the Southern Ocean between Marion and Amsterdam Island with a smaller hot spot showing up west of the Ross Ice Shelf (see Figure 15). For recently formed particles between three and ten nm diameter, (N_{3-10}), Figure 15 indicates potential source regions extending from the Indian sector between Marion and Amsterdam Island over Eastern Antarctic to Victoria Land. The lack of source indications for this size fraction over the rest of the Southern Ocean may be simply due to the sparse coverage of concurrent N_3 and N_{10} data. The identified potential source region comprises and confirms the source area over Antarctica identified by Humphries et al., (2016) albeit here with data from at least ten different years with at least 1000 trajectory points per geocell. We note that air masses from a belt reaching from Tasmania and Macquarie Island to Amsterdam Island less frequently led to very high values of (N_{3-10}) as compared to air masses with low number concentrations, again consistent with the findings of Humphries et al., (2016) who measured low particle number concentrations north of the atmospheric polar front. Finally, the potential source region for somewhat aged particles, (N_{10}), in Figure 15 is most strongly expressed over the Antarctic coastal region's Riiser-Larsen and Cosmonauts Seas with an extension over high Central Antarctica to Victoria Land. This extension can be interpreted as indicating the possibility of a upper tropospheric to stratospheric origin of these particles being carried with katabatic winds towards coastal Antarctica as indicated in the summer map of air parcel origin in Suzuki et al. (2013).

4. SUMMARY AND CONCLUSIONS

More than 40 years of aerosol data including concentrations of particle number and of nine major ions collected over the Southern Ocean and coastal stations have been aggregated and filtered with back trajectories to reduce the risk of influence from adjacent continents. Latitudinal, seasonal, and air mass analyses yielded the following results:

- Only $nssSO_4$, and to a lesser extent nssK, show a monotonous decrease from high tropical to extremely clean Antarctic levels as might be expected on a course from near-continental to remote polar marine atmospheric conditions.
- The latitude range between –45° and –60° stands out with remarkable relative or absolute maxima of particle number and chemical mass concentrations even though the most prominent marine biological aerosol precursor exhibits its zonal minima in this region.
- Seasonal statistics of most of the analyzed parameters clearly reflect the marine biological control with broad maxima during austral summer.
- The DMS-oxidation products $nssSO_4$ and MSA are suspected to stimulate NPF-events with episodic high concentrations of N_3 already in September and October with a subsequent broad summer maximum until February. Consistent with diatom blooms producing NH_3, a broad summer maximum also is observed for NH_4.
- The concentrations of the somewhat larger N_{10}-particles even exhibit their highest values south of –65° in March. During the same month nssCa that we suspect to derive from the OSM also shows highest monthly averages after a structured rise since October from low winter values.
- For $nssSO_4$ and MSA, nssCa, nssK, and particle number concentrations the most prominent source regions were found in high DMS-areas close to Antarctica, whereas the potential source regions of nssMg and NH_4 were located in part further north over the Southern Ocean. We hypothesize that in part oceanic structures may cause geographic differences in aerosol source regions (see e.g., Deacon, 1982).

Our results suggest two foci of subsequent aerosol studies over the Southern Ocean:

1. The region between –40° and –60 ° in order to understand the processes leading to the relative maxima in several aerosol parameters, in particular those related to the ocean surface microlayer, and
2. Aerosol studies south of –65° understand source regions and source processes of new particle formation.

DATA ACCESSIBILITY STATEMENTS

Already published data sets utilized in the present study are available in the utilized format from the corresponding author. Unpublished data sets should be requested from the respective principle investigators.

NOTES

1 To simplify the text, we disregard the charge symbols of all ionic components.

2 The complete oceanic coverage of the DMS climatology allows for higher latitudinal resolution than the sparse aerosol data.

3 Apparent inconsistencies between DMS-distribution, land mask and continental shorelines are due to the retransformation of the original DMS-maps of Hulswar et al., (2021) onto the polar stereographic map of the present study.

ACKNOWLEDGEMENTS

We gratefully acknowledge the arguments on seasonal meridional circulation changes provided by Vimo Tihma, Finnish Meteorological Institute. The authors would also like to acknowledge the Australian Bureau of Meteorology and CSIRO for their long-term and continued support of

the Kennaook Cape Grim Baseline Air Pollution Monitoring Station. RSH wishes to thank the CSIRO Marine National Facility (MNF) for its support in the form of sea time on RV Investigator, support personnel, scientific equipment and data management. We acknowledge the traditional owners of the land and sea where many of these measurements were undertaken. SS wishes to express his gratitude to L. P. Golobokova for her analysis of aerosol samples, as well as to a large number of operators who carried out measurements on different research cruises: Kabanov D.M., Polkin V.V., Turchinovich Yu.S. Gubin A.V., Lubo-Lesnichenko K.E., Prakhov A.N., Sidorova O.R., Terpugova S.A., Vlasov N.I., Zenkova P.N.

FUNDING INFORMATION

Shrivardhan Hulswar and colleagues of the Indian Institute of Tropical Meteorology, Pune, India generously shared their latest DMS-climatology with us before its publication. Aerosol data for the Indian coastal station, Maitri at Antarctica was made available by Vimlesh Pant and Devendraa Siingh of the Indian Institute of Tropical Meteorology, Pune, India which is funded by Ministry of Earth Sciences, Government of India. CPC-data from the Cape Point GAW station, South African Weather Service were contributed by Casper Labuschagne. Marek Kubicki shared the CPC data from the Polish station Arctowski in the South Shetlands with us. Willy Maenhaut of Ghent University kindly provided sample data from Amsterdam Island. We thank Alexander Mangold of the Royal Meteorological Institute of Belgium for providing the particle number concentration data for Princess Elisabeth Antarctica station. These measurements were financed by the Belgian Science Policy office through research contracts BR/143/A2/AEROCLOUD and BR/175/A2/CHASE and BR/175/A2/CHASE-2. Multiple datasets from island and coastal stations were made available by Greg Ayers, CSIRO, Australia, Joe Prospero of the University of Miami, USA, and Rolf Weller, Alfred Wegener Institute, Bremerhaven, Germany. Aerosol data from the first Circumantarctic research cruise ACE and from Bird Island were kindly shared by Julia Schmale, Extreme Environments Research Laboratory, Sion, Switzerland. Young Jun Yoon and Ki-Tae Park provided aerosol size distribution and major ion data collected at the Korean King Sejong Station, Antarctica. One of the authors (AKK) acknowledges the support of the Indian National Science Academy under the INSA Honorary Scientist Program. Silvia Becagli kindly contributed the chemical data from the Italian Antarctic station Mario Zucchelli, the collection of which had been supported by the Italian Ministry of University and Research and Programma Nazionale di Ricerca in Antartide through the Projects “Correlation between biogenic aerosol and primary production in the Ross Sea-BioAPRoS” (grant no. PNRA16_00065-A1).

COMPETING INTERESTS

The authors have no competing interests to declare.

AUTHOR AFFILIATIONS

Jost Heintzenberg
Institute for Tropospheric Research, Permoserstr. 15, 04318 Leipzig, Germany

Michel Legrand
Université Grenoble Alpes, CNRS, Institut des Géosciences de l’Environnement (IGE), Grenoble, France; Université Paris Cité and Univ Paris Est Creteil, CNRS, LISA, F-75013 Paris, France

Yuan Gao
Department of Earth and Environmental Sciences, Rutgers University, Newark, NJ USA

Keiichiro Hara
Fukuoka Univ. Faculty of Science, Department of Earth science system, Fukuoka

Shan Huang
Institute for Tropospheric Research, Permoserstr. 15, 04318 Leipzig, Germany; Institute for Environmental and Climate Research, Jinan University, Guangzhou, 511443, China

Ruhi S. Humphries
Climate Science Centre, CSIRO Oceans and Atmosphere, Melbourne, Australia; CSIRO Environment, Melbourne, Australia

Adarsh K. Kamra
Indian Institute of Tropical Meteorology, Pune, India

Melita D. Keywood
Climate Science Centre, CSIRO Oceans and Atmosphere, Melbourne, Australia; CSIRO Environment, Melbourne, Australia

Sergey M. Sakerin
V.E. Zuev Institute of Atmospheric Optics, Siberian Branch, Russian Academy of Sciences, Academician Zuev Square 1, 634021 Tomsk, Russia

REFERENCES

Aller, JY, Kuznetsova, MR, Jahns, CJ and **Kemp, PF.** 2005. The sea surface microlayer as a source of viral and bacterial enrichment in marine aerosols. *J. Aerosol Sci.,* 36: 801–812. DOI: https://doi.org/10.1016/j.jaerosci.2004.10.012

Alroe, J, Cravigan, LT, Miljevic, B, Johnson, GR, Selleck, P and **co-authors.** 2020. Marine productivity and synoptic meteorology drive summer-time variability in Southern Ocean aerosols. *Atmos. Chem. Phys.,* 20: 8047–8062. DOI: https://doi.org/10.5194/acp-20-8047-2020

Alvain, S. 2005. Étude de la distribution des principaux groupes de phytoplancton par télédétection satellitaire: Développement de la méthode PHYSAT à partir des données GeP&CO et application à l’archive SEAWIFS entre 1998 et 2004. In: *Climatologie*. Université Paris-Diderot – Paris VII.

Andreae, MO and **Crutzen, PJ.** 1997. Atmospheric Aerosols: Biogeochemical Sources and Role in Atmospheric Chemistry. *Science,* 276: 1052–1058. DOI: https://doi.org/10.1126/science.276.5315.1052

Arrigo, KR and **Dijken, GLV.** 2003. Phytoplankton dynamics within 37 Antarctic coastal polynya systems. *J. Geophys. Res.,* 108: 3271. DOI: https://doi.org/10.1029/2002JC001739

Arteaga, LA, Boss, E, Behrenfeld, MJ, Westberry, TK and **Sarmiento, JL.** 2020. Seasonal modulation of phytoplankton biomass in the Southern Ocean. *Nature Communications,* 11: 5364. DOI: https://doi.org/10.1038/s41467-020-19157-2

Asmi, E, Frey, A, Virkkula, AME, Manninen, H and **co-authors.** 2010. Hygroscopicity and chemical composition of Antarctic sub-micrometre aerosol particles and observations of new particle formation. *Atmos. Chem. Phys.*, 10. DOI: https://doi.org/10.5194/acpd-9-27303-2009

Ayers, GP and **Gras, JL.** 1991. Seasonal relationship between cloud condensation nuclei and aerosol methanesulphonate in marine air. *Nature*, 353: 834–835. DOI: https://doi.org/10.1038/353834a0

Ayers, GP, Bentley, ST, Ivey, JP and **Forgan, BW.** 1995. Dimethylsulfide in marine air at Cape Grim, 41°S. *J. Geophys. Res.,* 100: 21013–21021. DOI: https://doi.org/10.1029/95JD02144

Ayers, GP, Cainey, JM, Gillett, RW and **Ivey, JP.** 1997. Atmospheric sulphur and cloud condensation nuclei in marine air in the Southern Hemisphere. *Philos Trans R Soc Lond B Biol Sci,* 352: 203–211. DOI: https://doi.org/10.1098/rstb.1997.0015

Ayers, GP, Gillett, RW, Cainey, JM and **Dick, AL.** 1999. Chloride and bromide loss from sea-salt particles in Southern Ocean air. *J. Atmos. Chem.,* 33: 299–319. DOI: https://doi.org/10.1023/A:1006120205159

Ayers, GP, Ivey, JP and **Gillett, RW.** 1991. Coherence between seasonal cycles of dimethyl sulphide, methanesulphonate and sulphate in marine air. *Nature*, 349: 404–406. DOI: https://doi.org/10.1038/349404a0

Bates, TS, Calhoun, JA and **Quinn, PK.** 1992. Variations in the methanesulfonate to sulfate molar ratio in submicrometer marine aerosol particles over the South Pacific Ocean. *J. Geophys. Res.,* 97: 9859–9865. DOI: https://doi.org/10.1029/92JD00411

Brean, J, Dall'Osto, M, Simó, R, Shi, Z, Beddows, DCS and **co-authors.** 2021. Open ocean and coastal new particle formation from sulfuric acid and amines around the Antarctic Peninsula. *Nature Geosci.* DOI: https://doi.org/10.1038/s41561-021-00751-y

Charlson, RJ, Lovelock, JE, Andreae, MO and **Warren, SG.** 1987. Oceanic phytoplankton, atmospheric sulphur, cloud albedo and climate. *Nature*, 326: 655–661. DOI: https://doi.org/10.1038/326655a0

Chen, Q, Sherwen, T, Evans, M and **Alexander, B.** 2018. DMS oxidation and sulfur aerosol formation in the marine troposphere: a focus on reactive halogen and multiphase chemistry. *Atmos. Chem. Phys.,* 18: 13617–13637. DOI: https://doi.org/10.5194/acp-18-13617-2018

Chin, W-C, Orellana, MV and **Verdugo, P.** 1998. Spontaneous assembly of marine dissolved organic matter into polymer gels. *Nature*, 391: 568–572. DOI: https://doi.org/10.1038/35345

Cornwell, GC, Sultana, CM, Prank, M, Cochran, RE, Hill, TCJ and **co-authors.** 2020. Ejection of Dust From the Ocean as a Potential Source of Marine Ice Nucleating Particles. *J. Geophys. Res.*, 125. DOI: https://doi.org/10.1029/2020JD033073

Curtius, J. 2006. Nucleation of atmospheric aerosol particles. *Comptes Rendus Physique*, 7: 1027–1045. DOI: https://doi.org/10.1016/j.crhy.2006.10.018

Deacon, GER. 1982. Physical and biological zonation in the Southern Ocean. *Deep Sea Research Part A. Oceanographic Research Papers*, 29: 1–15. DOI: https://doi.org/10.1016/0198-0149(82)90058-9

Dreshchinskii, A and **Engel, A.** 2017. Seasonal variations of the sea surface microlayer at the Boknis Eck Times Series Station (Baltic Sea). *Journal of Plankton Research*, 39: 943–961. DOI: https://doi.org/10.1093/plankt/fbx055

Emmons, LK, Walters, S, Hess, PG, Lamarque, JF, Pfister, GG and **co-authors.** 2010. Description and evaluation of the Model for Ozone and Related chemical Tracers, version 4 (MOZART-4). *Geosci. Model Dev.*, 3: 43–67. DOI: https://doi.org/10.5194/gmd-3-43-2010

Frey, MM, Norris, SJ, Brooks, IM, Anderson, PS, Nishimura, K and **co-authors.** 2020. First direct observation of sea salt aerosol production from blowing snow above sea ice. *Atmos. Chem. Phys.*, 20: 2549–2578. DOI: https://doi.org/10.5194/acp-20-2549-2020

Garrett, WD. 1967. The organic chemical composition of the ocean surface. *Deep Sea Res.*, 14: 221–227. DOI: https://doi.org/10.1016/0011-7471(67)90007-1

Giglio, L, Randerson, JT and **van der Werf, GR.** 2013. Analysis of daily, monthly, and annual burned area using the fourth-generation global fire emissions database (GFED4). *Journal of Geophysical Research: Biogeosciences*, 118: 317–328. DOI: https://doi.org/10.1002/jgrg.20042

Gong, SL, Barrie, LA, Prospero, JM, Savoie, DL, Ayers, GP and **co-authors.** 1997. Modeling sea-salt aerosols in the atmosphere 2. Atmospheric concentrations and fluxes. *J. Geophys. Res.*, 102: 3819–3830. DOI: https://doi.org/10.1029/96JD03401

Gras, JL, Jimi, SI, Siems, ST and **Krummel, PB.** 2009. Postfrontal nanoparticles at Cape Grim: observations. *Environ. Chem.*, 6: 508–514. DOI: https://doi.org/10.1071/EN09075

Gras, JL, Podzimek, J, O'Connor, TC and **Enderle, KH.** 2002. Nolan-Pollak type CN counters in the Vienna aerosol workshop. *Atmos. Res.,* 62: 239–254. DOI: https://doi.org/10.1016/S0169-8095(02)00012-1

Hamilton, DS, Lee, LA, Pringle, KJ, Reddington, CL, Spracklen, DV and **co-authors.** 2014. Occurrence of pristine aerosol environments on a polluted planet. *PNAS*, 111: 18466. DOI: https://doi.org/10.1073/pnas.1415440111

Hara, K, Nishita-Hara, C, Osada, K, Yabuki, M and **Yamanouchi, T.** 2021. Characterization of aerosol number size distributions and their effect on cloud properties at Syowa Station, Antarctica. *Atmos. Chem. Phys. Discuss.*, 2021: 1–22. DOI: https://doi.org/10.5194/acp-2021-24

Hara, K, Osada, K, Yabuki, M, Matoba, S, Hirabayashi, M and **co-authors.** 2020. Atmospheric sea-salt and halogen cycles in the Antarctic. *Environmental Science: Processes & Impacts*, 22, 2003–2022. DOI: https://doi.org/10.1039/D0EM00092B

Hara, K, Sudo, K, Ohnishi, T, Osada, K, Yabuki, M and **co-authors.** 2019. Seasonal features and origins of carbonaceous aerosols at Syowa Station, coastal Antarctica. *Atmos. Chem. Phys.*, 19: 7817–7837. DOI: https://doi.org/10.5194/acp-19-7817-2019

Heintzenberg, J, Birmili, W, Wiedensohler, A, Nowak, A and **Tuch, T.** 2004. Structure, variability and persistence of the submicrometer marine aerosol. *Tellus,* 56B: 357–367. DOI: https://doi.org/10.1111/j.1600-0889.2004.00115.x

Heintzenberg, J, Covert, DS and **Van Dingenen, R.** 2000. Size distribution and chemical composition of marine aerosols: A compilation and review. *Tellus,* 52B: 1104–1122. DOI: https://doi.org/10.1034/j.1600-0889.2000.00136.x

Henley, SF, Cavan, EL, Fawcett, SE, Kerr, R, Monteiro, T and **co-authors.** 2020. Changing Biogeochemistry of the Southern Ocean and Its Ecosystem Implications. *Frontiers in Marine Science*, 7. DOI: https://doi.org/10.3389/fmars.2020.00581

Herenz, P, Wex, H, Mangold, A, Laffineur, Q, Gorodetskaya, IV and **co-authors.** 2019. CCN measurements at the Princess Elisabeth Antarctica research station during three austral summers. *Atmos. Chem. Phys.,* 19: 275–294. DOI: https://doi.org/10.5194/acp-19-275-2019

Hoffman, EJ and **Duce, RA.** 1977. Alkali and alkaline earth metal chemistry of marine aerosols generated in the laboratory with natural sea waters. *Atmos. Environ.*, 11: 367–372. DOI: https://doi.org/10.1016/0004-6981(77)90166-4

Hoffmann, EH, Tilgner, A, Schrödner, R, Bräuer, P, Wolke, R and **co-authors.** 2016. An advanced modeling study on the impacts and atmospheric implications of multiphase dimethyl sulfide chemistry. *PNAS*, 113: 11776–11781. DOI: https://doi.org/10.1073/pnas.1606320113

Huang, S, Wu, Z, Poulain, L, van Pinxteren, M, Merkel, M and **co-authors.** 2018. Source apportionment of the organic aerosol over the Atlantic Ocean from 53°N to 53°S: significant contributions from marine emissions and long-range transport. *Atmos. Chem. Phys.,* 18: 18043–18062. DOI: https://doi.org/10.5194/acp-18-18043-2018

Hulswar, S, Simo, R, Galí, M, Bell, T, Lana, A and **co-authors.** 2021. Third Revision of the Global Surface Seawater Dimethyl Sulfide Climatology (DMS-Rev3). *Earth Syst. Sci. Data Discuss.,* 2021: 1–56. DOI: https://doi.org/10.5194/essd-2021-236

Humphries, RS, Klekociuk, AR, Schofield, R, Keywood, M, Ward, J and **co-authors.** 2016. Unexpectedly high ultrafine aerosol concentrations above East Antarctic sea ice. *Atmos. Chem. Phys.,* 16: 2185–2206. DOI: https://doi.org/10.5194/acp-16-2185-2016

Jayarathne, T, Sultana, CM, Lee, C, Malfatti, F, Cox, JL and **co-authors.** 2016. Enrichment of Saccharides and Divalent Cations in Sea Spray Aerosol During Two Phytoplankton Blooms. *Environ Sci Technol*, 50: 11511–11520. DOI: https://doi.org/10.1021/acs.est.6b02988

Jiang, B, Xie, Z, Lam, PKS, He, P, Yue, F and **co-authors.** 2021. Spatial and Temporal Distribution of Sea Salt Aerosol Mass Concentrations in the Marine Boundary Layer From the Arctic to the Antarctic. *J. Geophys. Res.,* 126: e2020JD033892. DOI: https://doi.org/10.1029/2020JD033892

Johnson, MT and **Bell, TG.** 2008. Coupling between dimethylsulfide emissions and the ocean–atmosphere exchange of ammonia. *Environ. Chem.*, 5: 259–267. DOI: https://doi.org/10.1071/EN08030

Johnson, MT, Liss, PS, Bell, TG, Lesworth, TJ, Baker, AR and **co-authors.** 2008. Field observations of the ocean-atmosphere exchange of ammonia: Fundamental importance of temperature as revealed by a comparison of high and low latitudes. *Global Biochem. Cycles*, 22. DOI: https://doi.org/10.1029/2007GB003039

Junge, C. 1972. Our knowledge of the physico-chemistry of aerosols in the undisturbed marine environment. *J. Geophys. Res.*, 77: 5183–5200. DOI: https://doi.org/10.1029/JC077i027p05183

Keene, WC, Maring, H, Maben, JR, Kieber, DJ., Pszenny, AAP and **co-authors.** 2007. Chemical and physical characteristics of nascent aerosols produced by bursting bubbles at a model air-sea interface. *J. Geophys. Res.,* 112: D21202. DOI: https://doi.org/10.1029/2007JD008464

Keywood, MD, Ayers, GP, Gras, JL, Gillett, RW and **Cohen, D.** 1999. An evaluation of PM10 and PM2.5 size selective inlet performance using ambient aerosol. *Aerosol Sci. Technol.* 30: 401–407. DOI: https://doi.org/10.1080/027868299304589

Koga, S, Nomura, D and **Wada, M.** 2014. Variation of dimethylsulfide mixing ratio over the Southern Ocean from 36°S to 70°S. *Polar Science,* 8: 306–313. DOI: https://doi.org/10.1016/j.polar.2014.04.002

Koponen, IK, Virkkula, A, Hillamo, R, Kerminen, V-M and **Kulmala, M.** 2002. Number size distributions and concentrations of marine aerosols: Observations during a cruise between the English Channel and the coast of Antarctica. *J. Geophys. Res.,* 107. DOI: https://doi.org/10.1029/2002JD002533

Kremser, S, Harvey, M, Kuma, P, Hartery, S, Saint-Macary, A and **co-authors.** 2021. Southern Ocean cloud and aerosol data: a compilation of measurements from the 2018 Southern Ocean Ross Sea Marine Ecosystems and Environment voyage. *Earth Syst. Sci. Data*, 13: 3115–3153. DOI: https://doi.org/10.5194/essd-13-3115-2021

Kritz, MA and **Rancher, J.** 1980. Circulation of Na, Cl, and Br in the tropical marine atmosphere. *J. Geophys. Res.:*

Oceans, 85: 1633–1639. DOI: https://doi.org/10.1029/JC085iC03p01633

Lachlan-Cope, T, Beddows, DCS, Brough, N, Jones, AE, Harrison, RM and **co-authors.** 2020. On the annual variability of Antarctic aerosol size distributions at Halley Research Station. *Atmos. Chem. Phys.,* 20: 4461–4476. DOI: https://doi.org/10.5194/acp-20-4461-2020

Leck, C and **Bigg, EK.** 1999. Aerosol production over remote marine areas – A new route. *Geophys. Res. Lett.*, 23: 3577–3581. DOI: https://doi.org/10.1029/1999GL010807

Leck, C and **Bigg, EK.** 2005. Source and evolution of the marine aerosol – A new perspective. *Geophysical Research Letters*, 32: L19803. DOI: https://doi.org/10.1029/2005GL023651

Legrand, M, Ducroz, F, Wagenbach, D, Mulvaney, R and **Hall, J.** 1998. Ammonium in coastal Antarctic aerosol and snow: Role of polar ocean and penguin emissions. *J. Geophys. Res.*, 103: 11043–11056. DOI: https://doi.org/10.1029/97JD01976

Legrand, M, Preunkert, S, Wolff, E, Weller, R, Jourdain, B and **co-authors.** 2017. Year-round records of bulk and size-segregated aerosol composition in central Antarctica (Concordia site) – Part 1: Fractionation of sea-salt particles. *Atmos. Chem. Phys.*, 17: 14039–14054. DOI: https://doi.org/10.5194/acp-17-14039-2017

Legrand, M, Weller, R, Preunkert, S and **Jourdain, B.** 2021. Ammonium in Antarctic Aerosol: Marine Biological Activity versus Long-Range Transport of Biomass Burning. *Geophys. Res. Lett.,* 48: e2021GL092826. DOI: https://doi.org/10.1029/2021GL092826

Lewis, ER and **Schwartz, SE.** 2004. *Sea salt aerosol production: Mechanisms, methods, measurements and models – A critical review*. Washington DC, American Geophysical Union. DOI: https://doi.org/10.1029/GM152

Liss, PS and **Galloway, JN.** 1993. Air–sea exchange of sulphur and nitrogen and their interaction in the marine atmosphere. In: Wollast, R, Mackenzie, FT and Chou, L (eds.), *Interactions of C, N, P and S Biogeochemical Cycles and Global Change*, 259–281. Berlin: Springer. DOI: https://doi.org/10.1007/978-3-642-76064-8_11

Llort, J, Lévy, M, Sallée, J-B and **Tagliabue, A.** 2015. Onset, intensification, and decline of phytoplankton blooms in the Southern Ocean. *ICES Journal of Marine Science*, 72: 1971–1984. DOI: https://doi.org/10.1093/icesjms/fsv053

Lyons, B and **Pybus, MJS.** 1980. The seasonal variation in the nutrient chemistry of the surface microlayer of Galway Bay, Ireland. *Oceanol. Acta*, 3: 151–155.

Maenhaut, W, Zoller, WH, Duce, RA and **Hoffman, GL.** 1979. Concentration and size distribution of particulate trace elements in the south polar atmosphere. *J. Geophys. Res.,* 84: 2421–2431. DOI: https://doi.org/10.1029/JC084iC05p02421

McCoy, IL, Bretherton, CS, Wood, R, Twohy, CH, Gettelman, A and **co-authors.** 2021. Influences of Recent Particle Formation on Southern Ocean Aerosol Variability and Low Cloud Properties. *J. Geophys. Res.*, 126: e2020. DOI: https://doi.org/10.1029/2020JD033529

McMurry, PH. 2000. A review of atmospheric aerosol measurements. *Atmos. Environ.*, 34: 1959–1999. DOI: https://doi.org/10.1016/S1352-2310(99)00455-0

Mukherjee, P, Reinfelder, JR and **Gao, Y.** 2020. Enrichment of calcium in sea spray aerosol in the Arctic summer atmosphere. *Mar. Chem.,* 227. DOI: https://doi.org/10.1016/j.marchem.2020.103898

Nolan, PJ and **Pollak, LW.** 1946. The calibration of a photo-electric nucleus counter. *Proc. R. Ir. Acad.,* 51A: 9–31.

O'Dowd, CD, Davison, B, Lowe, JA, Smith, MH, Harrison, RM and **co-authors.** 1997. Biogenic sulphur emissions and inferred sulphate CCN concentrations in and around Antarctica. *J. Geophys. Res.*, 102: 12839–12854. DOI: https://doi.org/10.1029/96JD02749

Paulot, F, Jacob, DJ, Johnson, MT, Bell, TG, Baker, AR and **co-authors.** 2015. Global oceanic emission of ammonia: Constraints from seawater and atmospheric observations. *Global Biochem. Cycles*, 29: 1165–1178. DOI: https://doi.org/10.1002/2015GB005106

Peltola, M, Rose, C, Trueblood, JV, Gray, S, Harvey, M and **co-authors.** 2022. New particle formation in coastal New Zealand with a focus on open-ocean air masses. *Atmos. Chem. Phys.*, 22: 6231–6254. DOI: https://doi.org/10.5194/acp-22-6231-2022

Pirjola, L, O'Dowd, CDO, Brooks, IM and **Kulmala, M.** 2000. Can new particle formation occur in the clean marine boundary layer? *J. Geophys. Res.*, 105: 26531–26546. DOI: https://doi.org/10.1029/2000JD900310

Preunkert, S, Legrand, M, Jourdain, B, Moulin, C, Belviso, S and **co-authors.** 2007. Interannual variability of dimethylsulfide in air and seawater and its atmospheric oxidation by-products (methanesulfonate and sulfate) at Dumont d'Urville, coastal Antarctica (1999–2003). *J. Geophys. Res.*, 112. DOI: https://doi.org/10.1029/2006JD007585

Quinn, PK, Bates, TS, Johnson, JE, Covert, DS and **Charlson, RJ.** 1990. Interactions between the sulfur and reduced nitrogen cycles over the central Pacific ocean. *J. Geophys. Res.*, 95: 16405–16416. DOI: https://doi.org/10.1029/JD095iD10p16405

Raes, F. 1995. Entrainment of free tropospheric aerosols as a regulating mechanism for cloud condensation nuclei in the remote marine boundary layer. *J. Geophys. Res.*, 100: 2893–2903. DOI: https://doi.org/10.1029/94JD02832

Raphael, MN. 2007. The influence of atmospheric zonal wave three on Antarctic sea ice variability. *J. Geophys. Res.*, 112. DOI: https://doi.org/10.1029/2006JD007852

Righetti, D, Vogt, M, Gruber, N, Psomas, A and **Zimmermann, NE.** 2019. Global pattern of phytoplankton diversity driven by temperature and environmental variability. *Science Advances* 5. eaau6253. DOI: https://doi.org/10.1126/sciadv.aau6253

Riley, GA. 1963. Organic aggregates in seawater and the dynamics of their formation and utilization. *Limnol. Oceanogr.*, 8: 372–381. DOI: https://doi.org/10.4319/lo.1963.8.4.0372

Salter, ME, Hamacher-Barth, E, Leck, C, Werner, J, Johnson, CM and **co-authors.** 2016. Calcium enrichment in sea spray aerosol particles. *Geophys. Res. Lett.*, 43: 8277–8285. DOI: https://doi.org/10.1002/2016GL070275

Sanchez, KJ, Roberts, GC, Saliba, G, Russell, LM, Twohy, C and **co-authors.** 2021. Measurement report: Cloud processes and the transport of biological emissions affect southern ocean particle and cloud condensation nuclei concentrations. *Atmos. Chem. Phys.*, 21: 3427–3446. DOI: https://doi.org/10.5194/acp-21-3427-2021

Schmale, J, Baccarini, A, Thurnherr, I, Henning, S, Efraim, A and **co-authors.** 2019. Overview of the Antarctic Circumnavigation Expedition: Study of Preindustrial-like Aerosols and Their Climate Effects (ACE-SPACE). *Bull. Amer. Meteor. Soc.*, 100: 2260–2283. DOI: https://doi.org/10.1175/BAMS-D-18-0187.1

Schmale, J, Schneider, J, Nemitz, E, Tang, YS, Dragosits, U and **co-authors.** 2013. Sub-Antarctic marine aerosol: dominant contributions from biogenic sources. *Atmos. Chem. Phys.*, 13: 8669–8694. DOI: https://doi.org/10.5194/acp-13-8669-2013

Sciare, J, Mihalopoulos, N and **Dentener, FJ.** 2000. Interannual variability of atmospheric dimethylsulfide in the southern Indian Ocean. *J. Geophys. Res.*, 105: 26369–26377. DOI: https://doi.org/10.1029/2000JD900236

Sellar, AA, Jones, CG, Mulcahy, JP, Tang, Y, Yool, A and **co-authors.** 2019. UKESM1: Description and Evaluation of the U.K. Earth System Model. *Journal of Advances in Modeling Earth Systems*, 11: 4513–4558.

Shaw, GE. 1988. Antarctic aerosols: A review. *Rev. Geophys.*, 26: 89–112. DOI: https://doi.org/10.1029/RG026i001p00089

Shaw, GE, Benner, RL, Cantrell, W and **Clarke, AD.** 1998. On the regulation of climate: A sulfate particle feedback loop involving deep convection. *Clim. Change*, 39: 23–33. DOI: https://doi.org/10.1023/A:1005341506115

Simmons, JB, Humphries, RS, Wilson, SR, Chambers, SD, Williams, AG and **co-authors.** 2021. Summer aerosol measurements over the East Antarctic seasonal ice zone. *Atmos. Chem. Phys.*, 21: 9497–9513. DOI: https://doi.org/10.5194/acp-21-9497-2021

Simó, R. 2001. Production of atmospheric sulfur by oceanic plankton: biogeochemical, ecological and evolutionary links. *Trends in Ecology & Evolution*, 16: 287–294. DOI: https://doi.org/10.1016/S0169-5347(01)02152-8

Spracklen, DV, Pringle, KJ, Carslaw, KS, Chipperfield, MP and **Mann, GW.** 2005. A global off-line model of size-resolved aerosol microphysics: I. Model development and prediction of aerosol properties. *Atmos. Chem. Phys.*, 5: 2227–2252. DOI: https://doi.org/10.5194/acp-5-2227-2005

Stumm, W and **Morgan, JJ.** 1981. *Aquatic Chemistry*. New York NY, John Wiley & Sons.

Suzuki, K, Yamanouchi, T, Kawamura, K and **Motoyama, H.** 2013. The spatial and seasonal distributions of air-transport origins to the Antarctic based on 5-day backward trajectory analysis. *Polar Science*, 7: 205–213. DOI: https://doi.org/10.1016/j.polar.2013.08.001

Twohy, CH, DeMott, PJ, Russell, LM, Toohey, DW, Rainwater, B and **co-authors.** 2021. Cloud-Nucleating Particles Over the Southern Ocean in a Changing Climate. *Earth's Future*, 9: e2020EF001673. DOI: https://doi.org/10.1029/2020EF001673

van Loon, H. 1967. The Half-Yearly Oscillations in Middle and High Southern Latitudes and the Coreless Winter. *Journal of Atmospheric Sciences*, 24: 472–486. DOI: https://doi.org/10.1175/1520-0469(1967)024<0472:THYOIM>2.0.CO;2

Virkkula, A, Teinilä, K, Hillamo, R, Kerminen, V-M, Saarikoski, S and **co-authors.** 2006a. Chemical size distributions of boundary layer aerosol over the Atlantic Ocean and at an Antarctic site. *J. Geophys. Res.*, 111: D05306. DOI: https://doi.org/10.1029/2004JD004958

Virkkula, A, Teinilä, K, Hillamo, R, Kerminen, VM, Saarikoski, S and **co-authors.** 2006b. Chemical composition of boundary layer aerosol over the Atlantic Ocean and at an Antarctic site. *Atmos. Chem. Phys.*, 6: 3407–3421. DOI: https://doi.org/10.5194/acp-6-3407-2006

Wagenbach, D, Ducroz, F, Mulvaney, R, Keck, L, Minikin, A and **co-authors.** 1998. Sea-salt aerosol in coastal Antarctic regions. *J. Geophys. Res.*, 103: 10961–10974. DOI: https://doi.org/10.1029/97JD01804

Weisel, CP, Duce, RA, Fasching, JL and **Heaton, RW.** 1984. Estimates of the transport of trace metals from the ocean to the atmosphere. *J. Geophys. Res.*, 89: 11607–11618. DOI: https://doi.org/10.1029/JD089iD07p11607

Weller, R, Minikin, A, Petzold, A, Wagenbach, D and **König-Langlo, G.** 2013. Characterization of long-term and seasonal variations of black carbon (BC) concentrations at Neumayer, Antarctica. *Atmos. Chem. Phys.*, 13: 1579–1590. DOI: https://doi.org/10.5194/acp-13-1579-2013

Weller, R, Legrand, M and **Preunkert, S.** 2018. Size distribution and ionic composition of marine summer aerosol at the continental Antarctic site Kohnen. *Atmos. Chem. Phys.*, 18: 2413–2430. DOI: https://doi.org/10.5194/acp-18-2413-2018

Weller, R, Wagenbach, D, Legrand, M, Elsässer, C, Tian-Kunze, X and **co-authors.** 2011. Continuous 25-yr aerosol records at coastal Antarctica – I: Inter-annual variability of ionic compounds links to climate indices. *Tellus B*, 63: 901–919. DOI: https://doi.org/10.1111/j.1600-0889.2011.00542.x

Westberry, T, Behrenfeld, MJ, Siegel, DA and **Boss, E.** 2008. Carbon-based primary productivity modeling with vertically resolved photoacclimation. *Global Biochem. Cycles*, 22. DOI: https://doi.org/10.1029/2007GB003078

Wiedensohler, A, Orsini, D, Covert, DS, Coffmann, D, Cantrell, W and **co-authors.** 1997. Intercomparison study of the size-dependent counting efficiency of 26 condensation particle counters. *Aerosol Sci. Technol.*, 27: 224–242. DOI: https://doi.org/10.1080/02786829708965469

Wolff, EW, Legrand, MR and **Wagenbach, D.** 1998. Coastal Antarctic aerosol and snowfall chemistry. *J. Geophys. Res.*, 103: 10927–10934. DOI: https://doi.org/10.1029/97JD03454

Wulff, A, Iken, K, Quartino, LM, Al Handasl, A, Wiencke, C and **co-authors.** 2009. Biodiversity, biogeography and zonation of marine benthic micro- and macroalgae in the Arctic and Antarctic. *Botanica Marina*., 52: 491–507. DOI: https://doi.org/10.1515/BOT.2009.072

Xu, G, Gao, Y, Lin, Q, Li, W and **Chen, L.** 2013. Characteristics of water-soluble inorganic and organic ions in aerosols over the Southern Ocean and coastal East Antarctica during austral summer. *J. Geophys. Res*., 118: 13,303–313,318. DOI: https://doi.org/10.1002/2013JD019496

Yang, X, Frey, MM, Rhodes, RH, Norris, SJ, Brooks, IM and **co-authors.** 2019. Sea salt aerosol production via sublimating wind-blown saline snow particles over sea ice: parameterizations and relevant microphysical mechanisms. *Atmos. Chem. Phys*., 19: 8407–8424. DOI: https://doi.org/10.5194/acp-19-8407-2019

TO CITE THIS ARTICLE:
Heintzenberg, J, Legrand, M, Gao, Y, Hara, K, Huang, S, Humphries, RS, Kamra, AK, Keywood, MD and Sakerin, SM. 2023. Spatio-Temporal Distributions of the Natural Non-Sea-Salt Aerosol Over the Southern Ocean and Coastal Antarctica and Its Potential Source Regions. *Tellus B: Chemical and Physical Meteorology*, 75(1): 47–64. DOI: https://doi.org/10.16993/tellusb.1869

Submitted: 24 January 2023 **Accepted:** 12 September 2023 **Published:** 22 September 2023